

## Holographic refractive index detector for application in microchip-based separation systems

Norbert Burggraf<sup>†a,b</sup>, Beat Krattiger<sup>†a</sup>, Andrew J. de Mello<sup>c</sup>, Nico F. de Rooij<sup>b</sup> and Andreas Manz<sup>\*a,c</sup>

<sup>a</sup> Ciba-Geigy, Corporate Analytical Research, CH-4002 Basle, Switzerland

<sup>b</sup> Institute of Microtechnology, University of Neuchâtel, Rue A. L. Breguet 2, CH-2000, Neuchâtel, Switzerland

<sup>c</sup> Zeneca/SmithKline Beecham Centre for Analytical Sciences, Department of Chemistry, Imperial

College of Science, Technology and Medicine, Exhibition Road, South Kensington, London, UK SW7 2AY

**A novel detection scheme for capillary electrophoresis on planar glass microchips is presented. The application of a holographic-based refractive index detector to the electrophoretic separation of carbohydrates is described. The microchip device consists of a cyclic (square) separation channel having a circumference of 80  $\mu\text{m}$ , a width of 40  $\mu\text{m}$  and a depth of 10  $\mu\text{m}$ . The volume of the injection scheme is approximately 16 pl. Separation and refractive index detection of a mixture of sucrose, N-acetylglucosamine and raffinose, each at a concentration of 33 mM, was achieved within 17 s of injection. Preliminary results demonstrate the feasibility of using hologram-based refractive index detectors in microchip separation systems. Although the initial detection limits are poor in comparison with alternative techniques, the potential of a universal detector of this kind is clear.**

**Keywords:** Holographic refractive index detector; microchips; capillary electrophoresis; carbohydrates

Miniaturization of conventional laboratory instrumentation has been the focus of much attention during the last decade. The advantages of 'downsizing' analytical processes lie in improved efficiency with respect to sample size, response time, cost, throughput and automation. In particular, miniaturization of liquid phase separation methods has proved highly successful in the manipulation and analysis of small amounts of samples. This new generation of analytical instrumentation has been termed miniaturized total analysis systems ( $\mu$ -TAS).<sup>1,2</sup> A  $\mu$ -TAS aims to combine all steps of a complete, chemical analysis (sample handling, chemical reactions, sample separation, detection and product isolation) on a single, integrated device. Normally, such devices are fabricated on glass or silicon substrates using standard micromachining methods (photolithography, etching, thin-film deposition and bonding). The result is a planar chip containing an enclosed channel manifold through which the sample can be maneuvered. In addition, more complex components such as heaters, electrodes and mixers can be fabricated within the channel network.

A diversity of chemical separation techniques have been successfully integrated into the concept of a  $\mu$ -TAS. These include capillary electrophoresis (CE),<sup>3-6</sup> free-flow electrophoresis,<sup>7,8</sup> open-channel electrochromatography,<sup>9,10</sup> open-channel liquid chromatography,<sup>11-13</sup> gas chromatography,<sup>14</sup> micellar electrokinetic capillary chromatography<sup>15,16</sup> and synchronized cyclic capillary electrophoresis (SCCE).<sup>17-19</sup>

The adaptation of conventional detection protocols to measurement in small volumes has closely accompanied the development of  $\mu$ -TAS. Indeed, it has long been realized that size limits for  $\mu$ -TAS are primarily set by the system detector. For example, when performing CE on a typical microfabricated device, injection volumes typically range between  $10^{-14}$  and  $10^{-10}$  dm<sup>3</sup>. At a diagnostically relevant target concentration of 1 nM, this results in between 10 and  $10^4$  detectable molecules. Consequently, it is clear that high-sensitivity detection is essential when performing micro-separations.

Small volume detection in analytical technology has generally been based around optical measurements (either absorption or fluorescence). Unfortunately, small volume absorption measurements are compromised owing to the difficulty in probing small volume cells whilst maintaining a sufficiently long pathlength.<sup>20,21</sup> With microfabricated devices this problem is exacerbated (owing to reduced channel dimensions) and, to date, fluorescence methods have proved superior. Detection limits for fluorescence based measurements are extremely low.<sup>22</sup> As few as  $10^5$  molecules are generally detectable in most laboratories utilizing laser-induced fluorescence (LIF). Furthermore, recent developments in ultra-high sensitivity fluorescence detection have allowed single molecule detection to be performed 'on-chip'.<sup>23</sup> Although fluorescence techniques are inherently sensitive, they are costly and not applicable for all molecular systems (*i.e.*, not all species that absorb radiation fluoresce).

Other approaches to detection have included electrochemiluminescence,<sup>24</sup> electrochemical<sup>25</sup> and thermal conductivity methods.<sup>14</sup> For example, Arora *et al.*<sup>24</sup> recently demonstrated the detection of only  $3 \times 10^4$  tris(2,2'-bipyridyl)ruthenium(II) molecules in a 100 nl probe volume 'on-chip'. In addition, elegant experiments have demonstrated the feasibility of coupling electrophoresis microchips with the technique of electrospray ionization mass spectrometry (ESI-MS). Xue *et al.*<sup>26</sup> demonstrated high sensitivity (low nanomolar) microchip ESI-MS in the analysis of proteins whilst Ramsey and Ramsey<sup>27</sup> reported a method of generating electrospray from solutions emerging from microchannels etched on planar glass substrates. Both approaches extend the applicability of  $\mu$ -TAS to molecules that are non-fluorescent, and lead to the possibility of high-throughput MS analysis in screening and diagnostic applications.

The need for alternative detection protocols that are both sensitive and universal is apparent. Refractive index (RI) detection has been successfully applied to many analytical techniques (including HPLC<sup>28</sup> and CE<sup>29,30</sup>). RI based detectors have important characteristics which make them attractive alternatives to fluorescence and absorption methods. First, RI detection is a relatively simple technique useful in the micro- to millimolar range. It can be used with a wide variety of buffer systems, is universal in nature and is concentration sensitive

<sup>†</sup> Present address: Storz Endoskop GmbH, Schneckackerstrasse 1, CH-8200 Schaffhausen, Switzerland.

<sup>\*</sup> Present address: EG&G IC Sensors, 1701 McCarthy Blvd., Milpitas, CA 95035, USA.

(not mass sensitive). In addition, RI detectors have been shown to be successful in performing sensitive absorption detection in narrow bore capillaries (< 50  $\mu\text{m}$  id) using thermo-optical methods.<sup>29,31</sup>

The major challenge when applying RI detection to CE is controlling Joule heating. The variation of RI with temperature ( $dn/dT$ ) for most solvent systems is of the order of  $10^{-4}$  RI units (RIU)  $\text{K}^{-1}$  at room temperature. Since most applications require a sensitivity below  $\Delta n = 10^{-6}$  RIU, thermal stability becomes the dominant factor in lowering detection limits. This limitation is partly offset when moving to a microfabricated format.  $\mu$ -TAS for CE are conventionally fabricated by etching channels on a planar glass substrate. Channel dimensions are typically 10–20  $\mu\text{m}$  deep, 20–50  $\mu\text{m}$  wide and 10–100 mm long. These dimensions are significantly smaller than those of typical capillaries used in CE. During electrophoresis, solution resistance to current transport causes Joule heating. This can be considerable under normal conditions. Simple theory defines the heat generated per unit length ( $Q$ ) in rectangular channels as

$$Q = \frac{U^2 h^2 a}{L^2} \lambda c \quad (1)$$

where  $U$  (V) is the applied potential,  $h$  (m) is the channel height,  $a$  is the aspect ratio,  $\lambda$  ( $\text{m}^2 \text{mol}^{-1} \Omega^{-1}$ ) is the (pH-dependent) molar conductivity of the buffer and  $c$  ( $\text{mol dm}^{-3}$ ) its concentration. Eqn. (1) clearly demonstrates that a reduction in the cross-sectional area (and channel length) will minimize heat generation and thus temperature variations within the channel. This in turn will reduce variations in  $n$  and improve detector sensitivity.

A variety of RI detectors have been used in separation based analyses. Early attempts utilized interference patterns arising from side-illuminated capillaries. Optical interfaces within the capillary system separate the incident beam into three components (reflected, refracted and transmitted parts) which interfere in the far field and yield an interference pattern characteristic of sample in the detector volume. This method has been successfully applied to HPLC, CE and flow-injection analysis.<sup>29</sup>

The ‘off-axis’ method for CE was also demonstrated by Bruno *et al.*<sup>30</sup> in the analysis of underivatized sugars in a 50  $\mu\text{m}$  id capillary. They identified Joule heating as the major source of experimental noise. A more recent study by the same group used a holographic optical element to generate the interference pattern (rather than the capillary).<sup>32</sup> In this case the sampling arm of the interferometer traverses the capillary at its centre, where the optical path is longer and diffraction effects are smaller. This approach allowed the use of capillaries as narrow as 5  $\mu\text{m}$  id.

This paper extends the application of holographic optical elements (HOEs) and reports the first demonstration of a holographic RI detector applied to a microchip-based separation system. Preliminary results established the feasibility of RI detection for CE separations on planar glass microchips.

### Principle of refractive index detection

The principle of hologram-based RI measurement is shown in Fig. 1. A collimated, coherent beam of radiation is partially deflected by an HOE placed at a given angle (approximately  $30^\circ$ ) with respect to the illumination beam. The HOE acts as a set of two nearly superimposed focusing lenses, laterally displaced by a distance of 14  $\mu\text{m}$ . It acts to divide the incident beam into two coherent beams, and focus them on to the plane of the channel within the planar, glass substrate. One beam (probe beam) is directed through the electrophoresis channel and the second (reference beam) acts as a control and passes

through the glass substrate only. As indicated, both beams subsequently diverge in the far field and interfere. This results in the generation of an interference pattern consisting of equally spaced fringes, which are detected on a photodiode array (PDA). Interference occurs since both beams originate from the same source. A change in RI within the channel (*e.g.*, when an analyte band passes through the detector volume) induces a phase change in the probing beam, resulting in a lateral shift of the fringe pattern. A detailed description of theory is given elsewhere.<sup>32</sup>

## Experimental

### CE microchip

SCCE glass structures were used in these studies to perform CE owing to their availability.<sup>19</sup> All devices were fabricated under contract by Baumer IMT (Greifensee, Switzerland) using proprietary processes. Structures used in this work were made from soda lime glass (4012 SLW 5, Hoya, Tokyo, Japan). Channels were formed in the substrate material by etching with glycerol-HF solution. All channels were 10  $\mu\text{m}$  deep and 40  $\mu\text{m}$  wide. The isotropic etching procedure resulted in a rounded channel profile, with a channel bed width of 20  $\mu\text{m}$ . A cover plate was thermally bonded to the substrate by heating the assembly at 500  $^\circ\text{C}$  for 3 h, followed by 580  $^\circ\text{C}$  for 3 h. The complete device was then allowed to cool for at least 12 h. Ten holes drilled in the top plate allowed access to the fluidic network. The chip layout used is illustrated in Fig. 2. The volume of the injection scheme was approximately 12  $\mu\text{l}$ . As noted previously, the construct was only used to perform CE and not SCCE. Consequently, RI detection was performed in the locality of the asterisk. This corresponds to a separation length of approximately 20 mm or one quarter of the loop. The lengths of the inlet and injection channels were 10 and 12 mm, respectively.

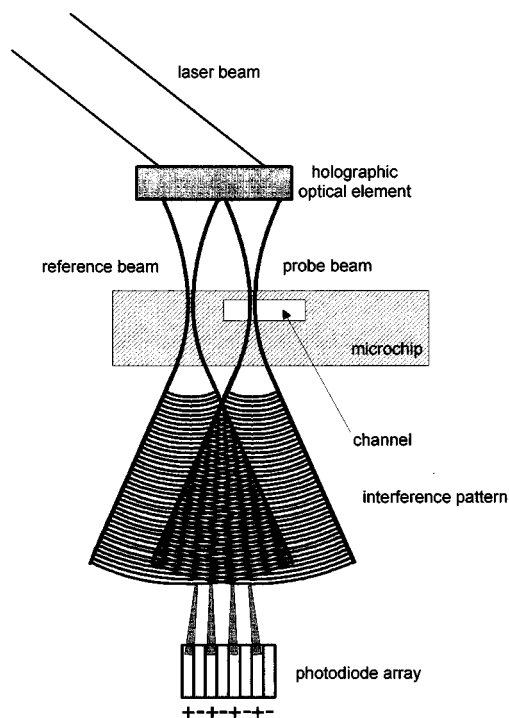


**Fig. 1** Principle of holographic RI detection: the HOE generates both reference and probe beams. Beams ‘fan out’ and interfere in the far field producing an evenly spaced fringe pattern. A change in the refractive index within the channel results in a shift of the fringe pattern.

### Optical system

The optical set-up for RI detection is shown in Fig. 3. Briefly, a diode laser module (LDM 145; Imatronic, Batavia, IL, USA) operating at 670 nm and 3 mW was used as the light source for all experiments. A lens was mounted at the front of the laser diode to collimate the laser output. A precision current source was used to drive the laser diode. The HOE was glued at an angle of 30° on a machined plastic pipe and connected to the laser diode. This acts to shield the laser output and to avoid Schlieren effects. All HOEs were manufactured according to standard photolithographic procedures, and had detection efficiencies ranging from 16 to 23% batch to batch. The laser diode was maintained at a constant temperature to ensure a stable laser output. This was achieved using a Peltier element (Melcor, Trenton, NJ, USA) and temperature controller (LDT 5901B; ILX Lightwave). The laser diode and HOE were mounted on a motor controlled  $x$ - $y$  translation stage (Spindler Hoyer, Göttingen, Germany). This allows for facile alignment of the probe and reference beams.

A cylindrical lens (Newport, Fountain Valley, CA, USA) was used to compress the interference pattern along one direction. The fringes were equally spaced and thus easily monitored by a

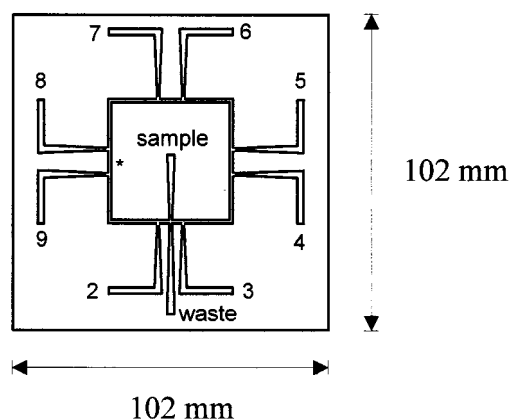


**Fig. 2** Layout of cyclic CE chip. The square separation channel has a circumference of 80 mm, a width of 40/20  $\mu\text{m}$  at the top/bottom and a depth of 10 mm. The volume of the injection scheme is approximately 16 pl.

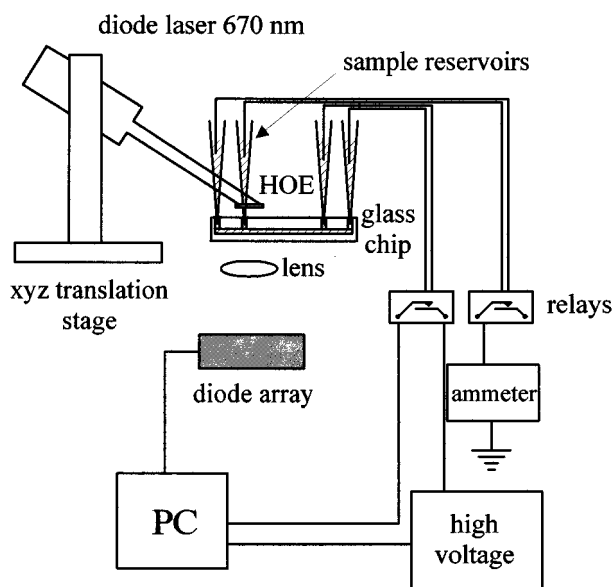


**Fig. 3** Schematic diagram of the experimental set-up showing the glass chip, reservoirs, electrodes, diode laser, HOE and diode array (not drawn to scale).

PDA (KOM 2045; Siemens, Fürth, Germany) mounted on an  $x$ - $y$  translation stage (Microbench; Spindler Hoyer). The PDA consisted of eight single diodes (four pairs) and was wired in parallel to combine the signals of the four fringes. With this set-up, the lateral shift of the fringe pattern caused by sample passing through the detection volume was converted into a voltage. An Apple Quadra computer was used to perform data acquisition and analysis.

### Capillary electrophoresis

Four (where necessary) high voltage power supplies (HCN 12500; FUG Elektronik, Rosenheim, Germany) were used to provide the high potentials for electrophoresis. They were connected to external electrolyte reservoirs by Pt electrodes. Current was monitored by an auto-ranging picoammeter (Model 485; Keithley, Cleveland, OH, USA) between a solvent reservoir and ground. All buffer reservoirs were connected to a high voltage power supply. Both the sample and waste reservoirs (of the injection channel) can be connected to high voltage power supplies in addition to ground. High voltage relays (Magnecraft, Chicago, IL, USA) were placed between the power supplies and electrodes. All relays were controlled by TTL signals generated by an Apple Quadra computer with a DAC (NB MIO 16 XH 18; National Instruments, Austin, TX, USA).

To obtain an evenly charged channel surface, the complete fluidic network was washed with 0.1 M NaOH prior to use. For separation, channels were pressure filled with buffer using nitrogen at 0.5 MPa. Injection was effected by electroosmotically filling the intersection zone of the square channel and the injection channel (expanded portion of Fig. 2). This was achieved by applying a voltage of 1000 V between the 'sample' and 'waste' reservoirs for 15 s. Subsequently, an applied voltage of 5 or 2.5 kV between reservoirs 9 and 5 allowed electrophoretic movement of sample along the separation channel.

### Reagents

Two buffer systems were used: a pH 9.0 buffer of 20 mM boric acid and 100 mM tris(hydroxymethyl)aminomethane (AnalaR grade) and a pH 9.0 buffer of 100 mM  $\text{B}(\text{OH})_3$  and 0.1 M NaOH. Sucrose, *N*-acetylglucosamine and raffinose (Fluka, Buchs, Switzerland) were used without further purification.

### Results

The feasibility of holographic RI detection for microchip based separation systems was established in two ways, as follows.

#### Injection and detection of a single component

Using the protocol outlined previously, a sample of 30 mM sucrose solution was injected on to the SCCE chip. Subsequent movement around the square channel was driven by an applied potential between reservoirs 9 and 5. The RI detector was positioned 20 mm along the separation channel (marked by an asterisk in Fig. 2). Fig. 4(a) shows the RI detector response as a function of time after injection for an electric field strength of 500  $\text{V cm}^{-1}$ . Although the S/N is poor, a distinct voltage peak at 6.68 s is observed. Fig. 4(b) shows a similar injection, but at an applied field strength of 1000  $\text{V cm}^{-1}$ . In this case the detection of the sucrose sample plug is observed after 3.54 s. Comparison of the figures demonstrates the fidelity of electroosmotic flow, since the detection time should be inversely proportional to the applied voltage.

Repetitive injection of four samples at each electric field strength (500 and 1000  $\text{V cm}^{-1}$ ) results in measurable values

describing the reproducibility of the geometrically defined injection process. These values are given in Table 1.

It can be seen that the reproducibility of the detection time is excellent and that the number of theoretical plates generated is satisfactory.

### Separation of a multi-component mixture

Fig. 5 shows the separation of a multicomponent mixture using an applied field strength of  $500 \text{ V cm}^{-1}$  and a separation length of 20 mm. The sample consists of a mixture of sucrose, *N*-acetylglucosamine and raffinose, each at a concentration of 33 mM and a pH of 9.0. All components are detected within 17 s of injection (sucrose, 13.3 s; *N*-acetylglucosamine, 14.8 s; raffinose, 16.3 s). Although the S/N is still unimpressive, all three components have been discriminated on the basis of their electrophoretic mobilities.

### Discussion

These preliminary results demonstrate the feasibility of using hologram-based RI detectors in microchip separation systems.

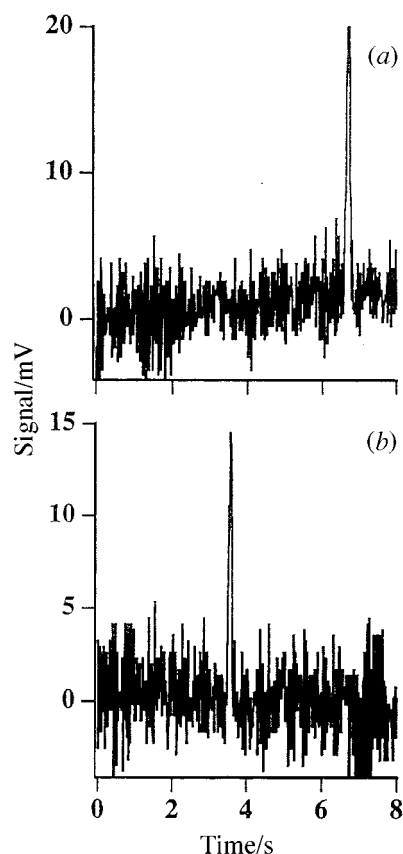


**Fig. 4** Injection of a sample of sucrose (30 mM) in 20 mM boric acid–100 mM Tris buffer (pH 9.0). RI detection with two different electric field strengths in the separation channel. Injection was performed using 1000 V for 15 s: (a) electric field strength,  $500 \text{ V cm}^{-1}$ ,  $L = 20 \text{ mm}$ ; (b) electric field strength,  $1000 \text{ V cm}^{-1}$ ,  $L = 20 \text{ mm}$ .

**Table 1** Reproducibility of the geometrically defined injection and separation process.

| Applied electric field/ $\text{V cm}^{-1}$ | $\sigma/s$       | $t_{\text{max}}/s$ | No. of theoretical plates |
|--|------------------|--------------------|---------------------------|
| 1000                                       | $0.02 \pm 0.002$ | $3.54 \pm 0.01$    | $31\,300 \pm 6\,300$      |
| 500  | $0.05 \pm 0.001$ | $6.68 \pm 0.01$    | $17\,800 \pm 700$         |

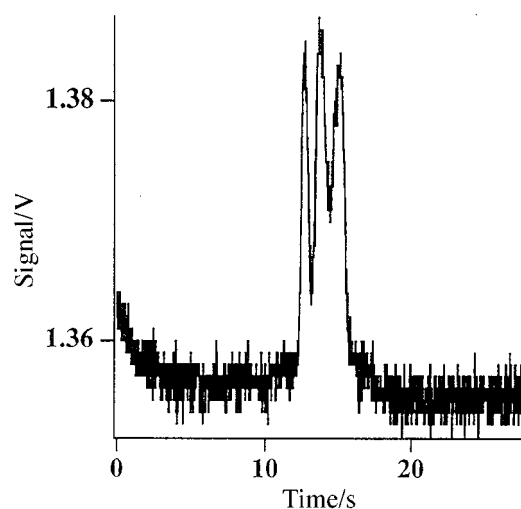


**Fig. 5** Electrophoretic separation of a mixture of three sugars (sucrose, *N*-acetylglucosamine and raffinose) at a concentration of 33 mM each. Electric field strength,  $500 \text{ V m}^{-1}$ ;  $L = 20 \text{ mm}$ .

It is clear that detection limits in the current system are barely sufficient for routine analysis (10 mM carbohydrate). However, it should be noted that this is a prototype system. In addition, injection of 20–30  $\mu\text{l}$  of sample corresponds to the detection of at most 600–900 fmol of carbohydrate.

Since RI detection is a concentration-sensitive protocol, the HOE RI detector should prove far more sensitive when applied to small volumes (picoliter and sub-picoliter) with time constants less than 10 ms. Current S/N levels will be improved through the use of electronic filtering and possibly temperature pulsing methods. It should also be noted that thermal lensing techniques have generated detection limits of single molecules in femtoliter volumes.<sup>33</sup> Assuming that the RI detector is ideally concentration sensitive, significantly improved detection limits should be attainable (through better chip design).

The hologram-based RI detection system presented in this paper is a most cost effective detection protocol. The complete detector is valued at a few hundred dollars, which compares well with current LIF and confocal detection schemes. More importantly, it should be possible to integrate the HOE on to the microchip. This would aid miniaturization and obviate the need for complex alignment of the detector and separation channel. In this way, multiple detectors could be integrated (*e.g.*, absorption, fluorescence and RI detection) to provide a truly universal detection unit.

The studies presented here are intended to be the first step towards a universal, small volume detector for chip-based separation systems. To that end, RI detection has been proved to be a feasible candidate for that eventual application.

We thank Alfredo Bruno, Sabeth Verpoorte (Novartis, Switzerland) and the group of Rene Dandliker (IMT Neuchâtel, Switzerland) for supplying us with the HOE for the experiments and the late H. Michael Widmer for long term support of research activities.

### References

- Manz, A., and Widmer, H. M., *Sens. Actuators, B*, 1990, **1**, 244.
- Manz, A., and Becker, H., *Microsystem Technology in Chemistry and Life Sciences*, Springer, Berlin, 1998.
- Manz, A., Harrison, J. D., Verpoorte, E., Fettingner, J. C., Paulus, A., Luedi, H., and Widmer, H. M., *J. Chromatogr.*, 1992, **593**, 253.

- 4 Jacobson, S. C., Hergenröder, R., Koutny, L. B., and Ramsey, J. M., *Anal. Chem.*, 1994, **66**, 1114.
- 5 Woolley, A. T., and Mathies, R. A., *Proc. Natl. Acad. Sci. USA*, 1994, **91**, 11 348.
- 6 Harrison, J. D., Manz, A., Fan, Z., Luedi, H., and Widmer, H. M., *Anal. Chem.*, 1992, **64**, 1926.
- 7 Raymond, D. E., Manz, A., and Widmer, H. M., *Anal. Chem.*, 1994, **66**, 2858.
- 8 Raymond, D. E., Manz, A., and Widmer, H. M., *Anal. Chem.*, 1996, **68**, 2515.
- 9 Jacobson, S. C., Hergenröder, R., Koutny, L. B., and Ramsey, J. M., *Anal. Chem.*, 1994, **66**, 2369.
- 10 He, B., and Regnier, F., *J. Pharm. Biomed. Anal.*, in the press.
- 11 Manz, A., Miyahara, Y., Miura, J., Watanabe, Y., Miyagi, H., and Sato, K., *Sens. Actuators, B*, 1990, **1**, 249.
- 12 Ocvirk, G., Verpoorte, E., Manz, A., Grasserbauer, M., and Widmer, H. M., *Anal. Methods Instrum.*, 1995, **2**, 74.
- 13 Cowen, S., and Craston, D. H., *Anal. Methods Instrum.*, 1996, Special Issue  $\mu$ -TAS '96, 196.
- 14 Terry, S. C., Jerman, J. H., and Angell, J. B., *IEEE Trans. Electron Devices*, 1979, **26**, 1880.
- 15 von Heeren, F., Verpoorte, E., Manz, A., and Thormann, W., *Anal. Chem.*, 1996, **68**, 2044.
- 16 Moore, A. W., Jacobson, S. C., and Ramsey, J. M., *Anal. Chem.*, 1995, **67**, 4184.
- 17 Burggraf, N., Manz, A., Effenhauser, C. S., Verpoorte, E., de Rooij, N. J., and Widmer, H. M., *J. High Resol. Chromatogr.*, 1993, **16**, 594.
- 18 Burggraf, N., Manz, A., Verpoorte, E., Effenhauser, C. S., and Widmer, H. M., *Sens. Actuators, B*, 1994, **20**, 103.
- 19 von Heeren, F., Verpoorte, E., Manz, A., and Thormann, W., *J. Microcol. Sep.*, 1996, **8**, 373.
- 20 Verpoorte, E., Manz, A., Lüdi, H., Bruno, A. E., Maystre, F., Krattiger, B., Widmer, H. M., van der Schoot, B. H., and de Rooij, N. F., *Sens. Actuators, B*, 1992, **6**, 66.
- 21 Liang, Z. H., Chiem, N., Ocvirk, G., Tang, T., Fluri, K., and Harrison, D. J., *Anal. Chem.*, 1996, **68**, 1040.
- 22 Barnes, M. D., Whitten, W. B., and Ramsey, J. M., *Anal. Chem.*, 1995, **67**, 418A.
- 23 Fister, J. C., Jacobson, S. J., Davis, L. M., and Ramsey, J. M., *Anal. Chem.*, 1998, **70**, 431.
- 24 Arora, A., de Mello, A. J., and Manz, A., *Anal. Comm.*, 1997, **34**, 393.
- 25 Woolley, A.T., Lao, K., Glazer, A. N., and Mathies, R. A., *Anal. Chem.*, 1998, **70**, 684.
- 26 Xue, Q., Foret, F., Dunayevskiy, Y. M., Zavracky, P. M., McGruer, N. E., and Karger, B. L., *Anal. Chem.*, 1997, **69**, 426.
- 27 Ramsey, R. S., and Ramsey, J. M., *Anal. Chem.*, 1997, **69**, 1174.
- 28 Bornhop, D. J., and Dovichi, N. J., *Anal. Chem.*, 1986, **58**, 504.
- 29 Bornhop, D. J., and Dovichi, N. J., *Anal. Chem.*, 1987, **59**, 1632.
- 30 Bruno, A. E., Krattiger, B., Maystre, F., and Widmer, H. M., *Anal. Chem.*, 1991, **63**, 2689.
- 31 Bruno, A. E., Paulus, A., and Bornhop, D. J., *Appl. Spectrosc.*, 1991, **45**, 462.
- 32 Krattiger, B., Bruin, G. J. M., and Bruno, A. E., *Anal. Chem.*, 1994, **66**, 1.
- 33 Takehiko, K., paper presented at the Eleventh International Symposium on High Performance Capillary Electrophoresis and Related Microscale Techniques, 1998.